Quantum yield bias in materials with lower absorptance

Van Dam, B.; Bruhn, B.; Kondapaneni, I.; Dohnal, G.; Wilkie, A.; Křivánek, J.; Valenta, J.; Mudde, Y.D.; Schall, P.; Dohnalová, K.

DOI
10.1103/PhysRevApplied.12.024022

Publication date
2019

Document Version
Final published version

Published in
Physical Review Applied

Quantum Yield Bias in Materials With Lower Absorptance

Bart van Dam,[1] Benjamin Bruhn,[1] Ivo Kondapaneni,[2] Gejza Dohnal,[3] Alexander Wilkie,[2] Jaroslav Křivánek,[2] Jan Valenta,[4] Yvo D. Mudde,[1] Peter Schall,[1] and Kateřina Dohnalová[1,*]

[1] *Institute of Physics, University of Amsterdam, Science Park 904, 1098 XH Amsterdam, Netherlands*

[2] *Faculty of Mathematics and Physics, Computer Graphics Group, KSVI, Charles University, Malostranské náměstí 25, Prague 1 CZ-11800, Czech Republic*

[3] *Faculty of Mechanical Engineering, Czech Technical University in Prague, Karlovo náměstí 13, 121 35 Prague 2, Czech Republic*

[4] *Department of Chemical Physics and Optics, Faculty of Mathematics and Physics, Charles University, Ke Karlovu 3, Prague 2 CZ-121 16, Czech Republic*

(Received 3 June 2019; published 12 August 2019)

Photoluminescence (PL) quantum yield (QY), which is defined as the ratio of emitted to absorbed photons, is the central quantity that characterizes light-emitting materials. It is an important parameter to assess the light efficiency of new materials, as well as identify novel photophysical mechanisms. While QY measurements are performed as standard in research and industry, accurate measurements are challenging. Here, we show that, besides known inaccuracies, PL QY measurements exhibit a surprising systematic bias. QY values are underestimated by a factor of two or more for samples with lower absorption, which can even lead to misinterpretation of results. We combine PL QY measurements of diluted Rhodamine 6G and two different semiconductor quantum dot solutions, via the standard integrating sphere method, with analytical modeling and ray-tracing simulations and find that, independent of the setup and luminescence mechanism, all measurements suffer from the same systematic underestimation of the QY. Through statistical analysis of the measured emitted and absorbed photon numbers, we uncover the origin of this underestimation in the asymmetry of the ratio distribution for low absorption, together with setup-specific features, such as signal offsets and nonlinearities. We suggest a robust calibration procedure to correct for this bias for precise evaluation of the QY in materials used for bioimaging, biosensing, and optoelectronic or photovoltaic devices.

DOI: 10.1103/PhysRevApplied.12.024022

I. INTRODUCTION

Photoluminescence (PL) quantum yield (QY) is an important parameter to quantify the emission efficiency, which is often used for the characterization of light-emitting materials and for the analysis of physical effects that could lead to improved performance, such as carrier multiplication or ligand stability in semiconductor quantum dots (QDs). The development of (nano)materials for optoelectronics and photovoltaics often encounters weakly absorbing materials, in the form of thin films or diluted solutions, requiring highly accurate and robust methodology for the evaluation of their photoluminescence efficiency. PL QY is defined as the ratio of emitted photons, N_{em}, to absorbed photons, N_{abs} [1–8],

$$\eta = \frac{N_{\mathrm{em}}}{N_{\mathrm{abs}}}, \tag{1}$$

and can be measured by a variety of techniques [1,2]. The integrating sphere (IS) method is most utilized because it yields absolute values without the need for a calibration standard. The IS method for QY measurements was first introduced in 1995 by Greenham [3] and later evolved from a three-step [4] to a two-step [5] measurement. This method enables the direct determination of the absolute number of emitted and absorbed photons [6,7] by comparing the calibrated emission and absorption spectra of the studied sample (s) to a suitable blank (ref) [Fig. 1(a)]:

$$\eta = \frac{N_s^* - N_{\mathrm{ref}}^*}{N_{\mathrm{ref}} - N_s} = \frac{\int^{\mathrm{em}} [I_s(\lambda) - I_{\mathrm{ref}}(\lambda)] C(\lambda) d\lambda}{\int^{\mathrm{exc}} [I_{\mathrm{ref}}(\lambda) - I_s(\lambda)] C(\lambda) d\lambda}, \tag{2}$$

where N and N^* denote the integrated intensities (numbers of photons) at the excitation and emission wavelengths, respectively; $I(\lambda)$ is the detected spectrum; and C is the correction factor for the spectral response of the detection system. The IS methodology is considered to be the most robust and reliable [1,8] and has been employed to study

*k.newell@uva.nl

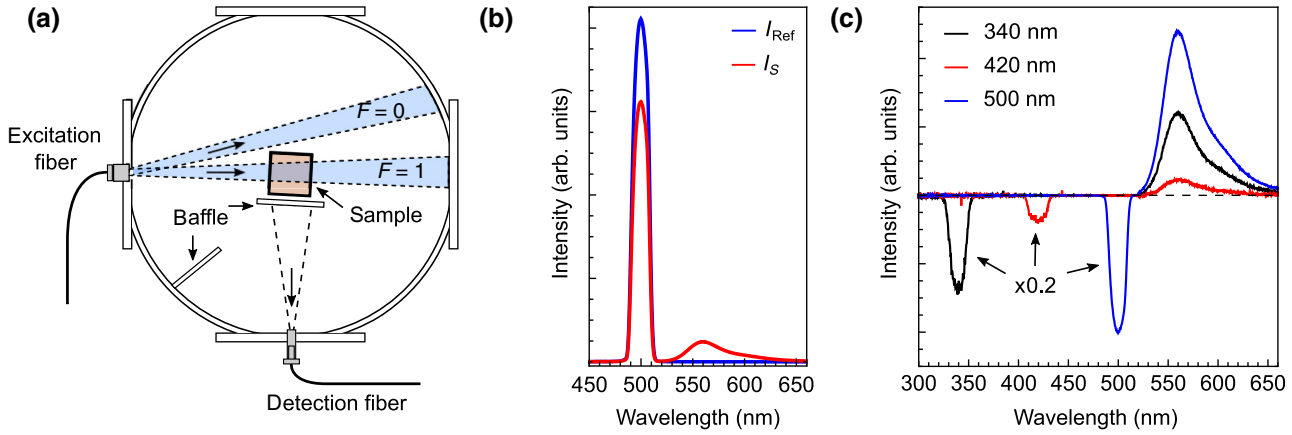

FIG. 1 (a) Schematic of "setup 1" for PL QY measurements using the IS technique (top cross-section view): The sample in the center of the sphere is excited directly by a fraction, F, of the incoming excitation beam [direct excitation ($F = 1$) and indirect excitation ($F = 0$) are shown]. Baffles prevent direct detection of the excitation and emission photons; see also Fig. S4 [41]. For comparative measurements, a setup with different geometry is used ("setup 2"), as described in Sec. II. (b) Examples of typical spectra for R6G in ethanol that are recorded with the reference (blue) and sample (red) inside the IS. (c) Three examples of spectra used for the evaluation of PL QY, which are obtained by subtracting sample and reference measurements for R6G in ethanol [such as those in panel (b)] at different excitation wavelengths.

a wide variety of materials and for the discovery of novel photophysical effects [9–18]. The IS method is also utilized by the lighting industry, where commercial devices based on the IS method for QY measurements can be purchased from several spectroscopic companies [19,20].

Multiple general guidelines for the IS PL QY methodology exist [1,2,21,22] and potential limitations of the technique, arising, e.g., from sample re(self-)absorption [23,24], excitation geometry [25], scattering [26], detection linearity [24], or PL of the IS wall material [27] have been addressed in detail. Several works have been dedicated to establishing a limit of the sample absorption beyond which QY can be reliably determined [21,28]. This limit is crucial because the absorption is directly linked to many experimental parameters, e.g., sample concentration, excitation wavelength, or volume, that may be varied in the study of a material. However, two effects have not yet been generally implemented in the QY methodology: first, signal offsets and nonlinearities for weak signals, which have been discussed only within the framework of IS measurements of absorption [7]; and, second, a systematic bias in QY measurement that occurs due to the skewed and even bimodal shape of the QY probability distribution function [29,30]. Importantly, this distribution function no longer has a defined meaning [30], making the situation even more complex.

Here, we investigate the applicability of the QY methodology experimentally for weakly absorbing samples and discover a surprising systematic bias that leads to an underestimation of the PL QY. We study diluted solutions of standard Rhodamine 6G dye (R6G) and two types of semiconductor QDs for comparison. We find a small constant shift that originates from reabsorption and, most importantly, a nonlinear systematic bias, which originates from two major contributions: the skewed shape of the QY distribution and small signal offsets and nonlinearities. These effects lead to a critical underestimation of the QY that depends on the sample's absorption, independent of the particular material type or setup geometry. We propose a calibration procedure that yields corrected QY values.

II. EXPERIMENTAL DETAILS

R6G from Sigma-Aldrich is dissolved in UV-grade ethanol (Merck KGaA, Uvasol), from which different concentrations are prepared by dilution. The concentration is estimated by comparison of the measured absorption coefficients with the value specified by Birge [31]. For all optical measurements, approximately 1.5 ml of solution is contained in a UV-spectroscopy-grade quartz cuvette (Hellma Analytics, 111-QS). CdSe/ZnSe/ZnS core-shell-shell QDs (CdSe QDs) in hexane are purchased from Center for Applied Nanotechnology (CAN) GmbH (CAN-dots Series A CSS). High-efficiency Si QDs are obtained from the group of Professor J.G.C. Veinot (Department of Chemistry, University of Alberta), which have been prepared by following the synthesis described in Refs. [32,33]. The concentration is estimated from the measured absorption coefficient and the absorption cross-sections reported in Ref. [34].

Transmittances of the sample (T_s) and reference (T_{ref}) are measured using a dual-beam spectrophotometer (Perkin Elmer, Lambda 950), from which the single-pass absorptance of the sample evaluated: $A = 1 - (T_s/T_{\mathrm{ref}})$.

For this, it is assumed that the reflectance of the sample and reference are the same.

For the determination of QY in "setup 1," we use a standard IS setup, as shown schematically in Fig. 1(a) and Fig. S4 within the Supplemental Material [41]. To illuminate our sample, we use a stabilized xenon lamp (Hamamatsu, L2273) coupled to a double-grating monochromator (Solar, MSA130). The excitation beam is split using a spectrally broad bifurcated fiber (Ocean Optics, BIF600-UV-VIS); we use one part to monitor fluctuations of the excitation intensity with a power meter (Ophir Photonics, PD300-UV) and the other part to excite the sample. We use a collimator lens to reduce the spot size at the sample position to enable direct excitation of the sample ($F = 1$). The samples are suspended, using an aluminum holder, in the center of the IS [internal walls made of Spectralon® (polytetrafluoroethylene), Newport, 70672] with a diameter of 10 cm. The use of such a type of holder is verified by ray-tracing simulations (see discussion with Fig. S6 [41]). Light is detected using a second spectrally broad optical fiber (Ocean Optics, QP1000-2-VIS-BX) coupled to a spectrometer (Solar, M266) equipped with a CCD (Hamamatsu, S7031-1108S). All measurements are corrected for the spectral response of the detection system, which we determine by illuminating the IS, via the excitation port, with a tungsten halogen calibration lamp (standard of spectral irradiance, Oriel, 63358) for the visible range and a deuterium lamp (Oriel, 63945) for the UV range (<400 nm). The measured calibration spectrum is corrected for the stray-light contribution of the spectrometer. QY is evaluated using Eq. (2). Reabsorption effects are corrected for by using the procedure described by Ahn *et al.* [23], by comparing the measured PL spectrum with that of a low-concentration sample for which reabsorption is negligible (dashed line in Fig. S1(b) [41]). Error estimates are obtained following the method of Chung *et al.* [35].

For QY measurements in "setup 2," we use an IS of 10 cm in diameter with an inner surface covered by the Spectraflect® coating. Excitation is provided by a laser-driven light source (LDLS, Energetiq, EQ-99X) coupled to the 15 cm monochromator (Acton SpectraPro SP-2150i). The monochromatized light (bandwidth of about 10 nm) is guided to the IS via a silica fiber bundle. The output signal from the IS is collected by another fused-silica fiber bundle placed in the direction perpendicular to the excitation axis and is shielded by three baffles against direct visibility to both the excitation source and the sample. The end of the fiber bundle (which has a stripelike shape) is imaged to the input slit of an imaging spectrograph (focal length of 30 cm), and a liquid-nitrogen-cooled CCD camera is used for detection. The spectral sensitivity of the complete apparatus is calibrated over the broad UV-near-infrared spectral range (300–1100 nm) using two radiation standards (Newport Oriel): a 45 W tungsten halogen lamp (above 400 nm) and a deuterium lamp (below 400 nm). Special attention is paid to avoiding stray-light effects in the spectrometer.

III. RESULTS AND DISCUSSION

For the PL QY measurements, we use the standard two-step IS technique (Fig. 1), validated by ray-tracing simulations (discussed in detail in the Supplemental Material [41]). We analyze three different light-emitting materials, an organic dye and two types of semiconductor QDs, over a broad range of absorptances. Absorptance is changed through variation in concentration, excitation wavelength, and/or sample thickness.

We first study a freshly made sample of R6G in ethanol; a commonly used calibration standard for comparative QY measurements, with a high QY of approximately 95% [36]. We prepare several solutions with concentrations between 6 and 120 μM. The spectral shape of the absorption coefficient of the R6G solution remains unaltered upon dilution (inset in Fig. S1(a) [41]), indicating the absence of material changes, such as clustering effects [37]. Also, the PL lifetime in the studied range is independent of excitation wavelength and concentration (Fig. S1(c) [41]), showing that the internal emission efficiency is constant throughout the studied range. To determine the PL QY, we compare the emission and transmission spectra of the sample (R6G in ethanol) to that of a reference (ethanol) [example in Fig. 1(b)]. From the difference [example in Fig. 1(c)], we obtain the total number of emitted and absorbed photons.

The absorptances and PL QYs for various R6G concentrations excited between 300 and 520 nm are shown in Fig. 2. As follows from the Kasha-Vavilov rule [31], R6G is expected to have a spectrally flat PL QY dependence. This is indeed observed for the higher concentration of 120 μM. However, solutions with lower R6G concentrations show excitation-wavelength-dependent QYs that drop, for some points, to as low as 38%. From a comparison of Figs. 2(a) and 2(b), it appears that the QY values roughly follow the spectral profile of the absorption of R6G (similarly for other panels). To investigate this possible relation, we replot all data from Fig. 2(b) against the single-pass absorptance of the sample in Fig. 2(c) and find a strong correlation: the QY values decrease in a nonlinear way with absorptance, and this occurs independently of whether the absorptance is lowered by the sample concentration or excitation wavelength. In particular, we find that, at absorptance values of $A_{\mathrm{crit}} \gtrsim 10-15\%$, the QY is constant and close to the expected literature value, but decreases nonlinearly for $A < A_{\mathrm{crit}}$. The same effect can be observed if both concentration and excitation wavelength are fixed and the single-pass absorptance of the R6G solution is decreased by changing the optical path length through the sample using a thinner cuvette, as shown in Figs. 2(d)–2(f). This suggests that the effect depends on the sample's absorption and not exclusively on

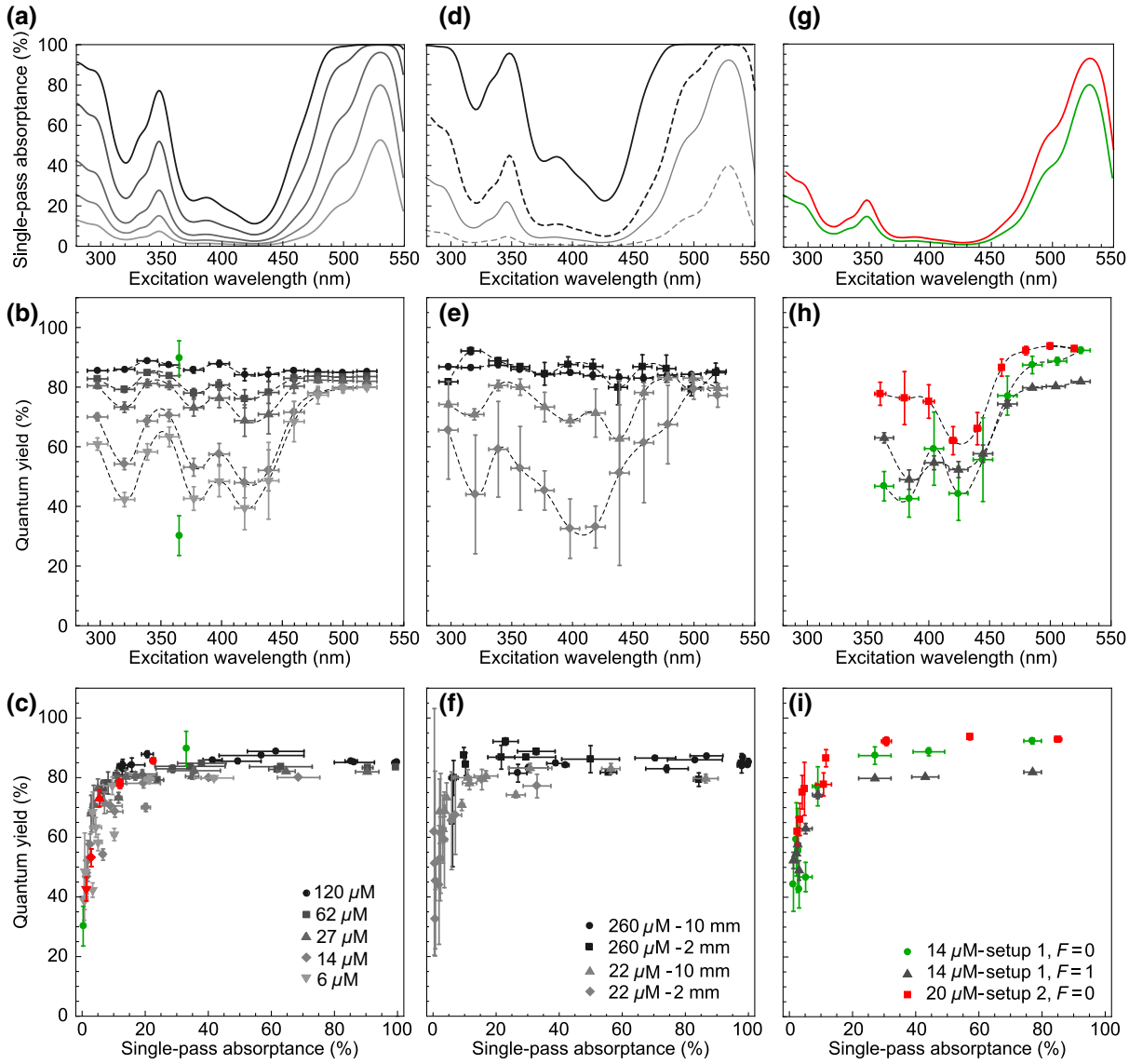

FIG. 2 The PL QY of R6G in ethanol for (a)–(c) varying excitation wavelength and concentration, (d)–(f) varying thickness of the cuvette (i.e., optical path length), and (g)–(i) direct and indirect excitation conditions measured in two different setups (setups 1 and 2, description in Sec. II). Legends in the bottom panels are the same for other related panels. The single-pass absorptances are shown in (a),(d),(g), and PL QY as a function of excitation wavelength are shown in (b),(e),(h) and replotted as a function of single-pass absorptance in (c),(f),(i). All data are corrected for reabsorption using the procedure described by Ahn *et al.* [23]. For comparison with the literature, the QY values determined by Faulkner [25] for 100 μM (the higher QY value) and 1 μM (the lower QY value) solutions of R6G in ethanol are plotted in (b),(c) in green.

the concentration, excitation wavelength, or optical path length. We carefully confirm this effect under different experimental conditions (Figs. 2(g)–2(i) and Fig. S2 [41]) and in a different experimental setup (Figs. 2(g)–2(i) and Fig. S3 [41]; "setup 2" is discussed in Sec. II). These measurements are in agreement with an observation in the literature, where a drop in QY for R6G has been also reported [25] [these data are, for comparison, shown in Figs. 2(b) and 2(c), green points].

The same effect is found for other commonly studied materials, such as suspensions of semiconductor QDs, specifically silicon QDs (Si QDs) and cadmium selenide QDs (CdSe QDs). Both materials have very different optical properties from each other and from those of R6G, such as emission efficiency and absorption and emission spectra [Fig. 3(a)]. The most notable difference between semiconductor QDs and fluorescent dye R6G is the broad featureless absorption spectrum, resulting from the bandlike dispersion in semiconductors. Also, Si QDs have a larger Stokes shift and a less abrupt absorption onset than that of CdSe QDs due to the indirect band structure. Furthermore, Si QDs have much more stable ligand

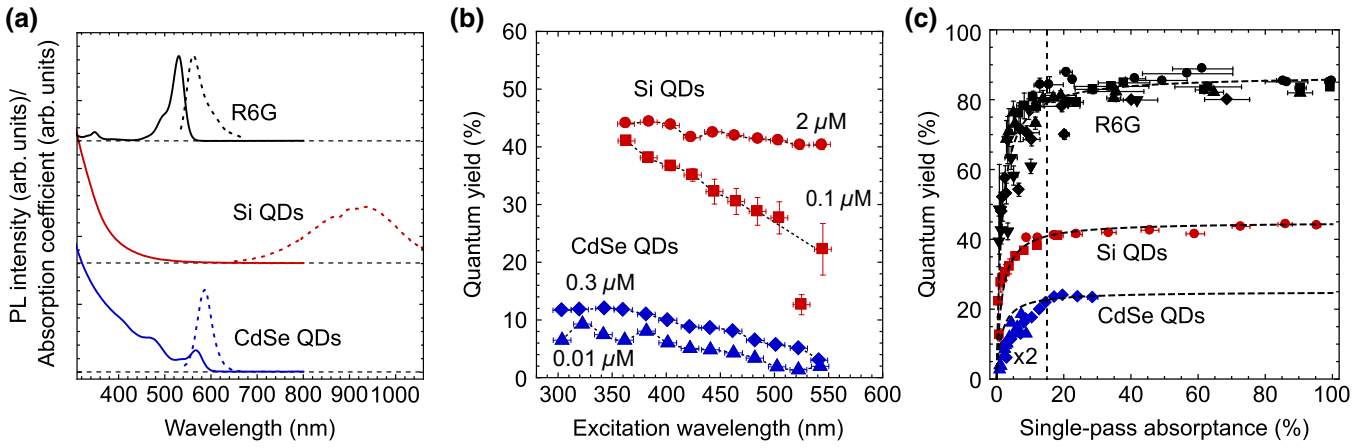

FIG. 3 (a) Absorption coefficients (full lines) and PL spectra (dashed lines) for R6G in ethanol (black), Si QDs in toluene (red), and CdSe QDs in hexane (blue). (b) PL QY dependence on the excitation wavelengths of CdSe QDs and Si QDs (the QY of the Si QDs below 360 nm is omitted, since the solvent is nontransparent in this spectral region). The dashed lines serve as guides to the eye. (c) PL QY from (b) replotted versus single-pass absorptance. For comparison, we add data for R6G from Fig. 2(c) (black symbols). The dashed lines serve as guides to the eye to emphasize the observed general trend of the QY. The critical absorptance value, A_{crit}, is indicated by the vertical dashed line.

capping, in comparison to that of CdSe QDs. Nonetheless, despite differences in absorption and emission, the effect is the same here—the PL QY of both types of QD materials decreases when the absorption decreases below A_{crit} [Fig. 3(c)], similarly to R6G (Fig. 2); this suggests that the observed excitation and concentration QY dependences are caused by the same effect. One might argue that, for semiconductor QDs, the process of emission and absorption is more complex than that for R6G, and therefore, the validity of the Kasha-Vavilov rule [31] might be weaker or not hold at all; this has led to various discussions of interesting novel physical phenomena in the recent literature [9–18]. The striking similarity in the behavior of R6G and the two types of QD materials indicates that the origin of the underestimation is the same, suggesting that a critical assessment and caution are required when interpreting such data, especially for samples absorbing below approximately 10%–15%.

To obtain an insight into this systematic absorption-related bias, we compare the experimental QY results with a traditionally used analytical model (AM) [4,5,21,25] and with numerical ray-tracing simulations (RTS). The AM approach describes the light inside the IS by uniformly distributed photon fluxes in a uniform IS geometry (Fig. S7 [41]). In this approach, the measured intensities, I^* and I in Eq. (2), are expressed in terms of the probability, p_x (Fig. S7 [29,41]), that emission and excitation light reach the detector port via multiple reflections inside the IS. In the RTS simulation, different photon paths are individually considered in a realistic IS setup, yielding solutions even for nonuniform photon distributions and IS geometries; this allows for more exact modeling of the setup (Figs. S4–S6). The resulting QY values obtained via modeling by AM and RTS approaches are shown in comparison with the experimental values from Fig. 2(c) in Fig. 4. The AM predicts a constant QY value, independent of absorption (black curve). The more realistic approach by the RTS (red symbols) also gives a constant QY, but with a slightly lower value of approximately 86%, which is in excellent agreement with our experimental measurements for high absorption (gray symbols). We find that this constant downshift of the PL QY is caused by a nonideal reflectivity of the sample holder material (aluminum); a similar constant downshift also arises from reabsorption, for which we correct these data using a procedure developed by Ahn *et al.* [23]. The rest of the setup and sample material properties influence the PL QY negligibly. Neither of the two approaches, however, explain the absorption-dependent decrease of the PL QY at low absorption (gray points in Fig. 4).

To elucidate the origin of this seeming decrease of QY, we measure the full distribution of QY values for low absorptances by repeated recording of photon numbers N_s, N_s^*, N_{ref}, and N_{ref}^* (Fig. S9 [41]). From this measurement, assuming a normal distribution of photon counts, we find an experimental uncertainty of 0.3%, which indicates a very precise measurement (we note that, in the limit of the low fluxes, one needs to take into account a Poisson distribution of photons, which, however, yields the same result [29]). We then compute QY values by taking random combinations of these values of N_s and N_{ref} into Eq. (2), and plot the resulting QY distribution in Fig. 5 (gray histograms). For the highest absorption of 20% [Fig. 5(a)], the QY distribution is narrow, symmetric, and centered around the expected value of approximately 75% (which becomes approximately 86% after correction for reabsorption [23]).

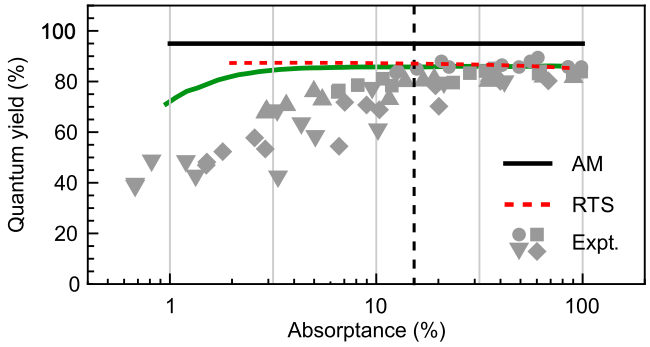

FIG. 4 Comparison of the experimental dependence of the PL QY of R6G on the single-pass absorptance (gray symbols) with simulated values from the AM (black line) and RTS (red symbols) approaches. For comparison, a peak value of the QY probability distribution [29] is also shown in the presence of measurement uncertainty in number of photons of $\alpha = 0.3\%$ (green line).

However, when the absorptance is lowered by moving the excitation wavelength off-resonance [Fig. 5(b)], by lowering the concentration [Fig. 5(c)], or both [Fig. 5(d)], the experimentally obtained QY histograms become broad and skewed. As a result, the most likely (peak) value of the QY shifts below the expected value observed for higher absorption; hence this leads to an underestimation of the QY. This effect can be as much as a factor of two or more for low-absorbing samples (see Figs. 2–5).

To further investigate the origin of this skewed distribution, we examine the measured number of emitted and absorbed photons separately as a function of single-pass absorptance [Fig. 6(a)]. We also plot the measured emission directly against the absorption [Fig. 6(b)]. While both AM and RTS approaches predict that both dependencies should be strictly linear and crossing the origin, the experimental data exhibit an offset of $A_{\text{off}} \sim 1.7\%$ for small absorptances. Figure 6(a) shows that the major contribution to this offset comes from the absorption. While the emission is typically evaluated against the background noise, the absorption is evaluated from a difference of two relatively strong transmission signals: one passing through the sample and the other passing through a reference. Hence, any subtle issue in the design of a "proper" reference material with respect to the sample might lead to an absorption offset. The inevitability of such experimental effects is demonstrated in some of the most precise IS measurements of absorption of pure water [7]. We observe this offset with small variations in all three types of samples studied here (Fig. S8 [41]). Interestingly, for the diluted CdSe QD sample, we even see a small offset in the emission signal (Fig. S8(b) [41]), which is probably linked to the ligand instability often reported for such systems [10,38–40], leading to material changes in diluted samples with respect to undiluted samples, and hence, to true changes in QY.

Taking into account these offsets, we can fit the QY probability distributions in Figs. 5(b)–5(e) analytically. To do so, we assume the measured photon counts follow a normal distribution, which is a fair assumption for the relatively strong signals encountered in QY measurements. The QY distribution function is then given by the ratio of two normal distributions, for which we have derived an

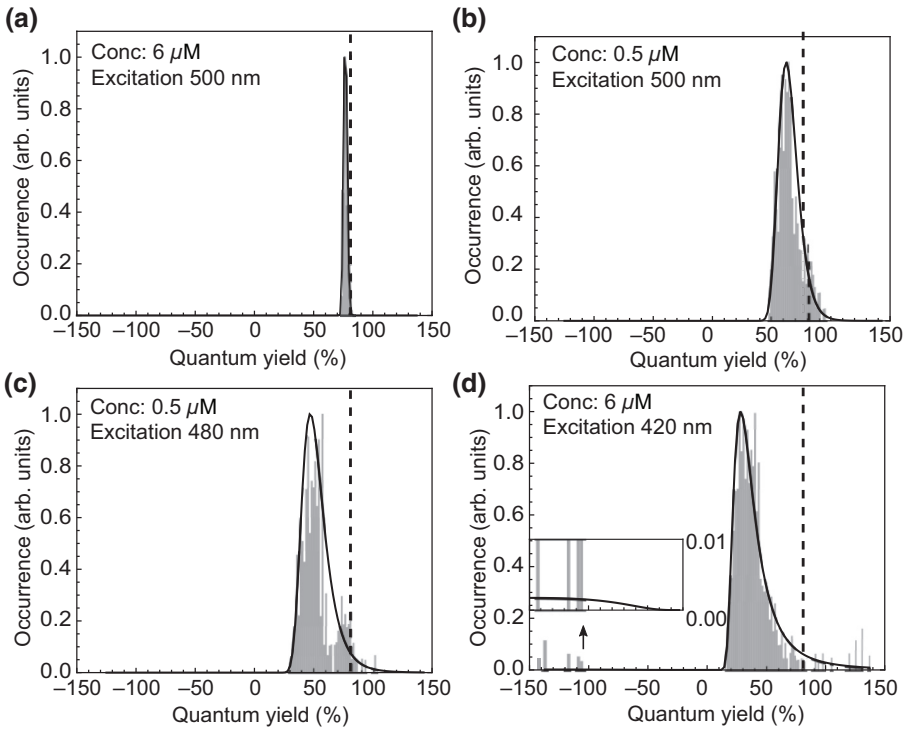

FIG. 5 Histograms of measured QY values of Rhodamine 6G in ethanol with a maximum QY of approximately 75% for different values of the single-pass absorptance (a) 20%, (b) 0.6%, (c) 2%, and (d) 0.8% (inset shows an enlargement of the negative QY range) achieved by varying sample concentration and excitation wavelengths (see the legends). The black solid line shows the fit using the ratio distribution for an experimental uncertainty of approximately 0.3% and experimental absorptance offset of approximately 1.7%. Dashed lines represent the measured value of the QY of approximately 81% [from Fig. 2(a)].

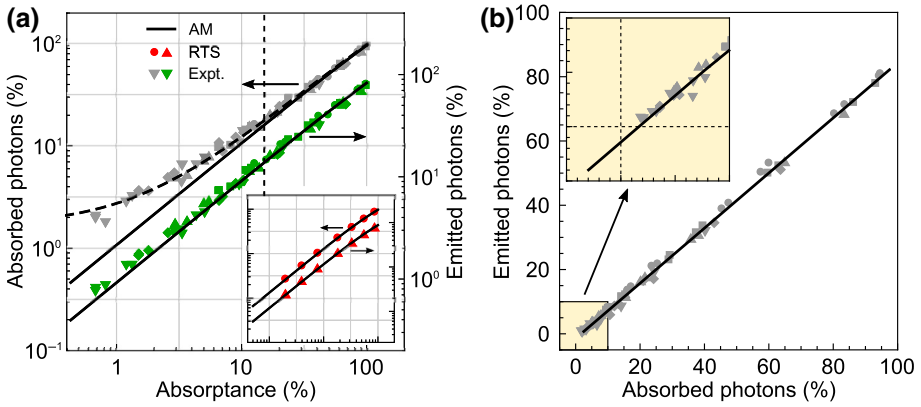

FIG. 6 (a) Experimentally determined dependences of the absorbed (gray symbols, left axis) and emitted (green symbols, right axis) photon fractions on the single-pass absorptance of the sample. The black line indicates the simulated dependence using the AM approach. The dashed curved line fits the experimental data with an absorption offset of 1.7%. The vertical straight dashed line indicates the position of A_{crit}. The inset shows a comparison of the AM approach (black lines) with the RTS approach for the fraction of absorbed (red circles) and emitted (red triangles) photons. Both approaches are in excellent agreement. (b) Linear dependence of the number of emitted and absorbed photons in the integrating sphere. The black line is a linear fit, the slope of which equals the ideal PL QY value. The inset shows an enlargement of the lowest signal range, unraveling small offset and nonlinearity.

analytical expression in Ref. [29]. As shown in Fig. 5, the measured QY histograms can indeed be fitted well by this derived analytical expression [29] for the measured experimental uncertainty of 0.3% (Fig. S9 [41]) and absorption signal offset of $A_{\mathrm{off}} \sim 1.7\%$ (Fig. 6); see the full black lines in Fig. 5. For low absorption, the denominator normal distribution is close to zero, which leads to a skewing of the ratio distribution, as shown in Figs. 5(b)–5(d). The peak value of the QY distribution function is plotted for more absorptance values in Fig. 4 (green).

The fit thus reproduces two main features very well: (i) the shift of the peak of the histogram from the ideal QY value, which increases for lower absorptances; and (ii) the shape of the distribution that is skewed and even bimodal with negative QY values [inset in Fig. 5(d)]. While the shape results from the ratio probability distribution functions alone [29], the shift itself is caused partly by the absorption offset of 1.7% and partly by the experimental uncertainty of 0.3%. Both effects are rather instrumental or methodology related. Their occurrence is setup and material independent, while the magnitude could vary (related to the offset and uncertainty magnitudes). Crucially, as the maximum of the resulting QY distribution does not coincide with the mean [29,30], averaging QY for low-absorbing samples does not yield the correct QY value, which is what we observe for three different systems in Figs. 2 and 3.

Combining our theoretical and experimental findings, we suggest a simple procedure that yields corrected QY values. Even though one can analyze the bias in detail following the steps described above, such an approach would be far too complex and time-consuming for routine use. Following our experience and findings, we suggest a simpler route, where one uses a high-quality reference material, such as a fresh solution of R6G dye to calibrate the setup. The idea is to measure a graph similar to that in Fig. 2(c), from which the critical absorption value, A_{crit}, for the specific QY setup can be determined. Please note that it is essential to take special care of reabsorption, possible lifetime changes, aggregation, etc. (see our detailed discussion above and in the Supplemental Material [41]). Thus, we need to measure the standard's QY dependence on the single-pass absorptance over a wide range of absorptances, at least between 1% and 30%, since A_{crit} can be expected to occur over a range of at least 5%–20% in a typical QY setup. Such a broad absorption range can be reached by varying independently (i) the excitation wavelength, (ii) the sample concentration, and (iii) the sample's optical thickness, or by a combination of the above, since the bias manifest independently of how the absorption is changed, as we show in Figs. 2 and 3. The critical absorption, A_{crit}, is then given by the single-pass absorptance at which the measured QY deviates from the expected constant value, as shown in Figs. 2(c), 2(f), 2(i), and 3(c). Finally, the QY of the sample of interest, $\eta_s^{\mathrm{meas}}(A)$, is measured and corrected for bias in the range $A < A_{\mathrm{crit}}$, using the QY dependence of the calibration standard, $\eta_{\mathrm{cal}}(A)$, with respect to the saturation value for $A > A_{\mathrm{crit}}$:

$$\eta_s^{\mathrm{cor}}(A) = \eta_s^{\mathrm{meas}}(A)\frac{\eta_{\mathrm{Cal}}(A > A_{\mathrm{crit}})}{\eta_{\mathrm{Cal}}(A)}. \tag{3}$$

We apply this correction procedure to the QY measurements presented in this paper [compiled for convenience in Fig. 7(a)] and show the results in Fig. 7(b). Indeed, the vast majority of the observed spectral and concentration dependences of the QY vanish, and are thus due to the described bias. For the particular example of CdSe QDs, a part of

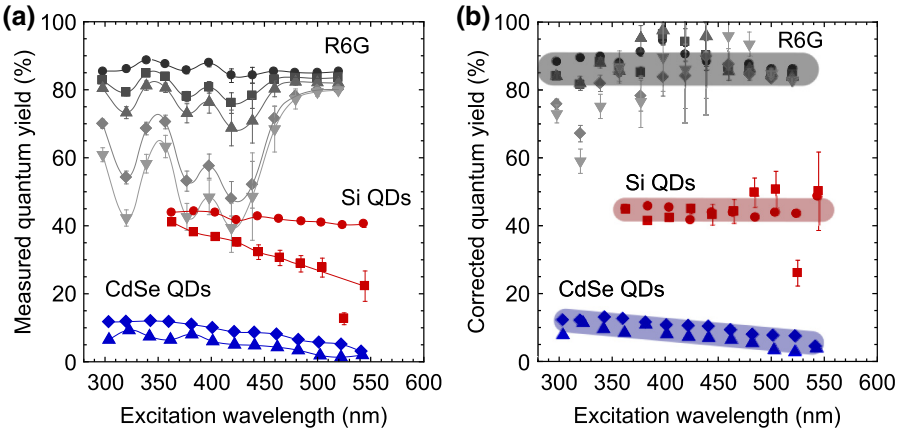

FIG. 7 QY versus excitation wavelength before (a) and after (b) correction for the absorption dependence of the QY methodology using Eq. (3). Different symbols represent different sample concentrations, as in Figs. 2 and 3. After correction, the QY of the Si QDs is constant at approximately 45% and independent of the sample concentration. Part of the excitation and concentration dependences of the QY of the CdSe QDs persists after correction, potentially related to instability of the ligands [10,38–40]. The correction function was obtained by taking a moving average of the QY versus single-pass absorption dependence of R6G in Fig. 2(c). For reference, the corrected QY for R6G is also shown.

the QY decrease remains after correction, which indicates some inherent physical QY effect that is not linked to bias. Thus, our proposed procedure corrects for bias and ensures reliable QY measurements over a broad range of experimental conditions and sample variations.

IV. CONCLUSION

Through an in-depth experimental study, we have uncovered a bias in QY measurements, leading to an underestimation of the PL QY for lower absorptances. This underestimation is rooted in the statistical distribution of absorbed and emitted photons, giving rise to a QY probability distribution that is skewed and bimodal for low absorption [29,30]. Also, setup- and sample-related effects play a role, such as reabsorption, nonideal sample holder material, or signal offsets and nonlinearities [7]. After careful analysis of these effects, we have successfully fitted the measured QY histograms obtained from repeated measurements. The role of these effects is often neglected in the literature, while QY is frequently used to characterize materials, such as semiconductor QDs, to study the emission efficiency dependence, e.g., on size [11,13] and density [12] of the QDs, excitation energy [9,14,15], or to show ligand instability [10]. Explicit QY dependence on various parameters has been interpreted in the past, in terms of novel effects [9–18], as a result of the size polydispersity of the QD ensembles, leading to a broadening of the emission spectrum [17], which, in turn, could lead to excitation-wavelength-dependent QY via excitation of different subsets of the QD ensemble; or one could argue that the concentration of the QD dispersions is expected to affect the QD interactions [9,14,18], which strongly depend on the interparticle distance. Our finding of a systematic bias of QY measurements indicates that care should be taken in the interpretation of these measurements and suggests plotting the QY of the QDs (or other materials) versus their single-pass absorptance to check for an underlying bias. If a nontrivial dependence occurs, our proposed procedure corrects for this intrinsic absorption dependence and eliminates the bias. In this way, it is possible to establish robust and reliable QY measurements for materials developed for, e.g., bio-imaging, biosensing, and optoelectronic or photovoltaic devices.

ACKNOWLEDGMENTS

The authors acknowledge Dutch STW funding (B.v.D, K.D.), FOM Projectruimte No. 15PR3230 (K.D.), MacGillavry Fellowship (K.D.); projects No. 16-22092S (J.V.), No. 18-12533S (A.W.), and No. 16-18964S (I.K., J.K.) of the Czech Science Foundation; and support from the ESIF, EU Operational Programme Research, Development and Education, and from the Center of Advanced Aerospace Technology (Grant No. CZ.02.1.01/0.0/0.0/16 019/0000826), Faculty of Mechanical Engineering, Czech Technical University in Prague (G.D.). The authors would like to thank Professor T. Gregorkiewicz (University of Amsterdam) for facilitating parts of this project, S. Regli and J. Veinot (University of Alberta, Canada) for providing the high-efficiency Si QD samples, I. Sychugov (KTH-Royal Institute of Technology) for an independent control measurement, and M. Hink (University of Amsterdam) for assistance with the time-resolved measurements. Finally, access to computing and storage facilities owned by parties and projects contributing to the National Grid Infrastructure MetaCentrum provided under the program "Projects

of Large Research, Development, and Innovations Infrastructures" (Grant No. CESNET LM2015042) is greatly appreciated.

B.v.D. carried out experimental measurements and analyzed the data. B.v.D., B.B., G.D., and K.D. performed simulations with the analytical model. I.K., A.W., and J.K. performed ray-tracing simulations. K.D., with Y.D.M., initiated this research and did preliminary experimental measurements. J.V. provided the independent experimental setup and analysis and initiated the use of the ray-tracing approach. P.S. and all the other authors have contributed to the final version of the manuscript.

[1] C. Würth, D. Geißler, T. Behnke, M. Kaiser, and U. Resch-Genger, Critical review of the determination of photoluminescence quantum yields of luminescent reporters, Anal. Bioanal. Chem. **407**, 59 (2015).

[2] G. A. Crosby and J. N. Demas, Measurement of photoluminescence quantum yields, J. Phys. Chem. **75**, 991 (1971).

[3] N. C. Greenham I, D. W. Samuel, G. R. Hayes, R. T. Phillips, Y. A. R. R. Kessener, S. C. Moratti, A. B. Holmes, and R. H. Friend, Measurement of absolute photoluminescence quantum efficiencies in conjugated polymers, Chem. Phys. Lett. **241**, 89 (1995).

[4] J. C. de Mello, H. F. Wittmannn, and R. H. Friend, An improved experimental determination of external photoluminescence quantum efficiency, Adv. Mater. **9**, 230 (1997).

[5] L. Mangolini, D. Jurbergs, E. Rogojina, and U. Kortshagen, Plasma synthesis and liquid-phase surface passivation of brightly luminescent Si nanocrystals, J. Lumin. **121**, 327 (2006).

[6] P. Elterman, Integrating cavity spectroscopy, Appl. Opt. **9**, 2140 (1970).

[7] R. M. Pope and E. S. Fry, Absorption spectrum (380–700 nm) of pure water. II. Integrating cavity measurements, Appl. Opt. **36**, 8710 (1997).

[8] C. Würth, M. Grabolle, J. Pauli, M. Spieles, and U. Resch-Genger, Relative and absolute determination of fluorescence quantum yields of transparent samples, Nat. Prot. **8**, 1535 (2013).

[9] D. Timmerman, J. Valenta, K. Dohnalová, W. D. A. M. de Boer, and T. Gregorkiewicz, Step-like enhancement of luminescence quantum yield of silicon nanocrystals, Nat. Nanotechnol. **6**, 710 (2011).

[10] M. Greben, A. Fucikova, and J. Valenta, Photoluminescence quantum yield of PbS nanocrystals in colloidal suspensions, J. Appl. Phys. **117**, 144306 (2015).

[11] M. L. Mastronardi, F. Maier-Flaig, D. Faulkner, E. J. Henderson, C. Kubel, U. Lemmer, and G. A. Ozin, Size-dependent absolute quantum yields for size-separated colloidally-stable silicon nanocrystals, Nano Lett. **12**, 337 (2012).

[12] J. B. Miller, A. R. Van Sickle, R. J. Anthony, D. M. Kroll, U. R. Kortshagen, and E. K. Hobbie, Ensemble brightening and enhanced quantum yield in size-purified silicon nanocrystals, ACS Nano **6**, 7389 (2012).

[13] W. Sun, C. Qian, L. Wang, M. Wei, M. L. Mastronardi, G. Casillas, J. Breu, and G. A. Ozin, Switching-on quantum size effects in silicon nanocrystals, Adv. Mater. **27**, 746 (2015).

[14] J. Valenta, M. Greben, S. Gutsch, D. Hiller, and M. Zacharias, Effects of inter-nanocrystal distance on luminescence quantum yield in ensembles of Si nanocrystals, Appl. Phys. Lett. **105**, 243107 (2014).

[15] S. Saeed, E. M. L. D. de Jong, K. Dohnalova, and T. Gregorkiewicz, Efficient optical extraction of hot-carrier energy, Nat. Commun. **5**, 4665 (2014).

[16] N. X. Chung, R. Limpens, and T. Gregorkiewicz, Photoluminescence quantum yield in ensembles of Si nanocrystals, Adv. Opt. Mater. **5**, 1600709 (2017).

[17] S. Miura, T. Nakamura, M. Fujii, M. Inui, and S. Hayashi, Size dependence of photoluminescence quantum efficiency of Si nanocrystals, Phys. Rev. B **73**, 245333 (2006).

[18] R. Limpens, A. Lesage, P. Stallinga, A. N. Poddubny, M. Fujii, and T. Gregorkiewicz, Resonant energy transfer in Si nanocrystal solids, J. Phys. Chem. C **119**, 19565 (2015).

[19] Horiba Quanta-phi, www.horiba.com/scientific/marketing-us/quantaphi/.

[20] Hamamatsu C9920-02G, https://www.hamamatsu.com/us/en/product/category/5001/5009/5032/C9920-02G/index.html.

[21] J. Valenta, Determination of absolute quantum yields of luminescing nanomaterials over a broad spectral range: From the integrating sphere theory to the correct methodology, Nanosci. Methods **3**, 11 (2014).

[22] C. Würth, M. Grabolle, J. Pauli, M. Spieles, and U. Resch-Genger, Comparison of methods and achievable uncertainties for the relative and absolute measurement of photoluminescence quantum yields, Anal. Chem. **83**, 3431 (2011).

[23] T. S. Ahn, R. O. Al-Kaysi, A. M. Müller, K. M. Wentz, and C. J. Bardeen, Self-absorption correction for solid-state photoluminescence quantum yields obtained from integrating sphere measurements, Rev. Sci. Instrum. **78**, 086105 (2007).

[24] C. Würth, C. Lochman, M. Spieles, J. Pauli, K. Hoffman, T. Schuttrigkeit, T. Franzl, and U. T. Resch-Genger, Evaluation of a commercial integrating sphere setup for the determination of absolute photoluminescence quantum yields of dilute dye solutions, Appl. Spectr. **64**, 733 (2010).

[25] D. O. Faulkner, J. J. Mcdowell, A. J. Price, D. D. Perovic, N. P. Kherani, and G. A. Ozin, Measurement of absolute photoluminescence quantum yields using integrating spheres - Which way to go?, Laser Photonics Rev. **6**, 802 (2012).

[26] C. Würth and U. Resch-Genger, Determination of photoluminescence quantum yields of scattering media with an integrating sphereâĂŕ: Direct and indirect illumination, Appl. Spectr. **69**, 749 (2015).

[27] J. Valenta, Photoluminescence of the integrating sphere walls, its influence on the absolute quantum yield measurements and correction methods, AIP Adv. **8**, 105123 (2018).

[28] S. Leyre, E. Coutino-Gonzalez, J. J. Joos, J. Ryckaert, Y. Meuret, D. Poelman, P. F. Smet, G. Durinck, J. Hofkens, G. Deconinck, and P. Hanselaer, Absolute determination of

photoluminescence quantum efficiency using an integrating sphere setup, Rev. Sci. Instrum. **85**, 123115 (2014).

[29] B. van Dam, G. Dohnal, B. Bruhn, and K. Dohnalova, Limits of emission quantum yield determination, AIP Adv. **8**, 085313 (2018).

[30] B. van Dam, G. Dohnal, B. Bruhn, and K. Dohnalova, Response to "Comment on 'Limits of emission quantum yield determination'", AIP Adv. **9**, 039102 (2019).

[31] S. J. Wawilow, Die Fluoreszenzausbeute von Farbstoffflösungen als Funktion der Wellenlänge des anregenden Lichtes. II, Z. Physik **42**, 311 (1927).

[32] J. A. Kelly and J. G. C. Veinot, An investigation into near-UV hydrosilylation of freestanding silicon nanocrystals, ACS Nano **4**, 4645 (2010).

[33] C. M. Hessel, E. J. Henderson, and J. G. Veinot, Hydrogen silsesquioxaneâĂŤ: A molecular precursor for nanocrystalline Si-SiO_2 composites and freestanding hydride-surface-terminated silicon nanoparticles, Chem. Mater. **18**, 6139 (2006).

[34] J. Valenta, M. Greben, Z. Remeš, S. Gutsch, D. Hiller, and M. Zacharias, Determination of absorption cross-section of Si nanocrystals by two independent methods based on either absorption or luminescence, Appl. Phys. Lett. **108**, 023102 (2016).

[35] N. X. Chung, R. Limpens, and T. Gregorkiewicz, in *Proceedings Volume 9562, Next Generation Technologies for Solar Energy Conversion VI* (2015), p. 95620O.

[36] R. F. Kubin and A. N. Fletcher, Fluorescence quantum yields of some rhodamine dyes, J. Lumin. **27**, 455 (1982).

[37] C. Würth, M. G. Gonzales, R. Niessner, U. Panne, C. Haisch, and U. Resch-Genger, Determination of the absolute fluorescence quantum yield of rhodamine 6G with optical and photoacoustic methods - Providing the basis for fluorescence quantum yield standards, Talanta **90**, 30 (2012).

[38] M. Grabolle, M. Spieles, V. Lesnyak, N. Gaponik, A. Eychmuller, and U. Resch-Genger, Determination of the fluorescence quantum yield of quantum dots: Suitable procedures and achievable uncertainties, Anal. Chem. **81**, 6285 (2009).

[39] J. De Roo, M. Ibanez, P. Geiregat, G. Nedelcu, W. Walravens, J. Maes, J. C. Martins, I. Van Driessche, M. V. Kovalenko, and Z. Hens, Highly dynamic ligand binding and light absorption coefficient of cesium lead bromide perovskite nanocrystals, ACS Nano **10**, 2071 (2016).

[40] O. E. Semonin, J. C. Johnson, J. M. Luther, A. G. Midgett, A. J. Nozik, and M. C. Beard, Absolute photoluminescence quantum yields of IR-26 Dye, PbS, and PbSe quantum dots, J. Phys. Chem. Lett. **1**, 2445 (2010).

[41] See Supplemental Material at http://link.aps.org/supplemental/10.1103/PhysRevApplied.12.024022 which contains supporting experimental evidence and details over ray tracing simulations.